

## Investigation of microstructural change and damping behaviour of Zn–27Al–1Cu alloy in different aging periods

*Zn–27Al–1Cu alaşımının farklı yaşlandırma periyotlarında mikroyapısal değişiminin ve darbe davranışının incelenmesi*

Fatih ŞENASLAN\*<sup>1,a</sup>, Murat AYDIN<sup>2,b</sup>

<sup>1</sup> Gümüşhane University, Engineering and Natural Sciences Faculty, Department of Mechanical Engineering, 29100, Gümüşhane

<sup>2</sup>Karadeniz Technical University, Engineering Faculty, Department of Mechanical Engineering, 61080, Trabzon

• Geliş tarihi / Received: 07.10.2021

• Düzeltilecek geliş tarihi / Received in revised form: 22.02.2022

• Kabul tarihi / Accepted: 28.02.2022

### Abstract

The ternary Zn–27Al–1Cu alloy is produced from raw materials by the gravity casting method. The produced alloy was subjected to aging after solutionizing and quenching. The effect of aging at different periods on the microstructure and damping behaviour of the alloy was investigated. The microstructural investigations revealed that the microstructure of the alloy in the as-cast state consisted of aluminium(Al)-rich  $\alpha$  dendrites surrounded by eutectoid  $\beta$  phase, and zinc(Zn)-rich  $\eta$  phase and copper(Cu)-rich  $\epsilon$  phase. The heat treatment eliminated the dendritic microstructure of the casting alloy and transformed it into a coarse-grained ( $\beta$ -matrix) stable form containing Zn-rich and Cu-rich precipitates. The microstructural changes after aging process were directly affected the mechanical properties of the alloy. The hardness and tensile strength increased with increasing ageing time up to 2.5 hours, but the percent elongation decreased. When the aging time reached 5 hours, hardness and tensile strength decreased while percent elongation increased significantly. The impact energy, namely toughness, increased in the early stage of aging, reduced sharply with increasing aging time and remained stable with a small increase in the prolonged stage of aging. The highest impact energy was attained from the aged alloy for 0.5 hours. The variation in damping energy was dependent on the changes in microstructural and mechanical properties caused by different aging periods. The prolonged aging process transformed the fracture characteristic of the as-cast alloy from relatively brittle to ductile fracture.

**Keywords:** Aging, Damping behaviour, Microstructure, Precipitation hardening, Zn–Al alloys

### Öz

Üçlü Zn–27Al–1Cu alaşımı, hammaddelerden kokil kalıba döküm yöntemiyle üretildi. Üretilen alaşım, çözündürme ve su verme işlemlerinden sonra yaşlandırmaya tabi tutuldu. Farklı periyotlarda yaşlandırmanın alaşımın mikroyapısı ve darbe davranışı üzerindeki etkisi incelendi. Mikroyapısal incelemeler, döküm halindeki alaşımın mikroyapısının alüminyumca (Al) zengin  $\alpha$  dendritleri ve onları çevreleyen ötektoid  $\beta$  fazı, çinkoca (Zn) zengin  $\eta$  fazı ve bakırca (Cu) zengin  $\epsilon$  fazından oluştuğunu ortaya çıkarmıştır. Isıl işlem döküm alaşımının dendritik mikroyapısını ortadan kaldırdı ve alaşımın mikroyapısını Zn ve Cu bakımından zengin çökeltiler içeren iri taneli ( $\beta$ -matrisli) kararlı bir forma dönüştürdü. Yaşlandırma işlemi sonrası oluşan mikroyapısal değişimler, alaşımın mekanik özelliklerini doğrudan etkilemiştir. Yaşlandırma süresinin 2,5 saate kadar artmasıyla sertlik ve çekme dayanımı artmış, ancak yüzde uzama azalmıştır. Yaşlandırma süresi 5 saate ulaştığında sertlik ve çekme dayanımı azalırken, yüzde uzama önemli ölçüde artmıştır. Darbe enerjisi, diğer bir ifade ile tokluk yaşlanmanın erken evresinde arttı, yaşlanma süresinin artmasıyla keskin bir şekilde azaldı ve uzun süreli yaşlandırma durumunda az bir artışla sabit kaldı. En yüksek darbe enerjisi 0,5 saat boyunca yaşlandırılmış alaşımdan elde edildi. Darbe enerjisindeki değişim, farklı periyotlarda yaşlandırma işleminden kaynaklanan mikroyapısal ve mekanik özelliklerdeki değişikliklere bağlıydı. Uzun süreli yaşlandırma işlemi, döküm durumundaki alaşımın kırılma karakteristiğini nispeten gevrek kırılmadan sünek kırılmaya dönüştürdü.

**Anahtar kelimeler:** Yaşlandırma, Darbe davranışı, Mikroyapı, Çökelme sertleşmesi, Zn-Al alaşım

\*a Fatih ŞENASLAN; fsenaslan@gumushane.edu.tr, Tel: (0456) 233 10 00, orcid.org/0000-0003-0498-6332

<sup>b</sup> orcid.org/0000-0002-8998-1620

## 1. Introduction

### 1. Giriş

Zinc-aluminium (Zn–Al) alloys have been generally operated as journal bearing materials because of their excellent tribological properties load-bearing performances for many years (Prasad, 2004; Babic et al., 2010; Anjan & Kumar, 2019). Conventional Zn–Al-based alloys also have been used for various engineering applications and industrial areas such as automobile engine parts, agricultural equipment, general hardware, work tools (Aydın, 2012; Anjan & Kumar, 2019; Pola et al. 2020). Some commercially used alloys are called ZA–8, ZA–12, ZA–27 and Alzen 501. Among the zinc-aluminium family, ZA-27 alloy has the highest strength, low density and superior bearings along with good wear resistance properties (Owoyeet al., 2019). The Zn–Al-based alloys are more preferred due to their outstanding properties in most mechanical and tribological applications than ferrous and nonferrous materials. These properties can be listed as easy production, low-cost, exceptional cast-ability, marvellous surface quality, easy machinability, high damping behaviour, and superior wear resistance properties (Savaşkan et al., 2002; Zhu et al., 2006; Yang et al., 2009; Pola et al. 2020). However, some mechanical properties of these alloys are not sufficient for advanced engineering applications and new manufacturing areas, particularly in the as-cast state. This situation seriously restricts the use of these alloys in industry. To eliminate or minimize these problems and develop the mechanical properties of the Zn–Al-based alloys, various methods have been applied until now (Pürçek et al 2005; Nagavelly et al., 2017; Aydın & Şenaslan, 2018; Movahedi et al., 2019; Zhang et al., 2020; Venc1 et al. 2021). It has been found that the best influential method for improving the strength of the binary alloy is the contribution of alloying elements such as Si, Ni, and Cu. These alloying elements lead to distortion in the Zn-Al matrix due to their very hard nature and increase the hardness and strength of the alloy. The increase in the strength of the Zn-Al based alloy with the presence of these alloying elements is mainly due to solid solution hardening and the formation of new phases. Liu et al. (2021) reported that the hardness of the Zn-12Al based alloy increased with the addition of Si increasing up to 1.2 wt. % due to silicon particles being harder than the matrix, but that when the Si content exceeded 0.3 wt. %, the impact energy of the alloy was distinctly reduced due to the splitting effect of silicon particles on the matrix. Choudhury et al. (2002) reported that the improvement in hardness and wear resistance of

the Zn-Al alloy modified with Ni (up to 0.9 wt. %) was due to the presence of the Ni<sub>3</sub>Al phase formed throughout the matrix. It found that the addition of copper in the range of 1–3 wt. % improves the strength and hardness of the Zn-Al alloys while reducing the ductility, due to solid solution hardening and the formation of relatively hard intermetallic  $\epsilon$  (CuZn<sub>4</sub>) and T' (Al<sub>4</sub>Zn<sub>3</sub>Cu) phases (Jeshvaghani et al., 2016). Some researchers have designed a series of typical alloys such as Zn–15Al–1Cu (Rollez et al., 2017), Zn–21Al–2Cu (Hernández-Rivera et al., 2017), Zn–25Al–3Cu (Savaşkan & Tan, 2015), Zn–26Al–1.5Cu–0.9Ni (Choudhury et al., 2002), Zn–27Al–3Si (Mao et al., 2015), Zn–38Al–2.5Cu–0.55Si (Ting et al., 2016) and Zn–40Al–2Cu–2Si (Savaşkan et al. 2021), apart from the commercial ZA alloys. However, some researchers (Turhal & Savaşkan 2003; Krupiński et al., 2018) indicated that the high addition of alloy elements deteriorated the structural stability and mechanical properties of Zn-Al alloys, such as dimensional instability, low strength and/or ductility. Heat treatments such as homogenization, stabilization and quench-aging are some of the most effective methods of eliminating dimensional instability and/or improving mechanical properties. Homogenization can be performed to achieve chemical homogeneity and to reduce micro-segregation in as-cast alloys by diffusion of atoms (Kai et al., 2017). Stabilization is used to greatly improve the dimensional stability of as-cast alloys. Quench-aging consists of three stages in which the alloys are subjected to solution treatment followed by rapidly cooling (quenching) and aging, to obtain the desired structural, physical and mechanical properties. However, in this heat treatment, the aging time and temperature play an important role in the structural and mechanical properties of the alloy. Thus, it is very important to determine the appropriate temperature and time parameters to obtain the desired properties in the alloy. Yang et al. (2013) examined the effect of heat treatment (at different temperatures and times) on the structural and mechanical properties of the ZA–27 alloy. They found that aging at low temperatures causes precipitation of very fine phases that reduce the ductility of the alloy, and furthermore, hardness and tensile strength decrease with increasing aging time, while aging at 140°C gives the highest ductility and tensile elongation, over 25%. Movahedi et al. (2019) fabricated ZA–27 syntactic foams using the counter-gravity infiltration casting method and investigated the effect of heat treatment (T7) on ZA–27 microstructure and mechanical properties. They reported that heat-treatment improved the specific energy absorption,

plateau stress, and energy absorption due to the change of the microstructure by increasing the ductility of the alloy. Zhang et al. (2020) found that after heat treatments, which are subjected to solution treatment at different temperatures (ranging from 280 °C to 400 °C) for different times (ranging from 1h to 3h) followed by water quench, all original phases and structures dissolved completely and the newly formed ZA-22 alloy merely consisted of sub-micron granular eutectoid structure. In addition, the significantly increased interface density and the change in the  $\alpha/\eta$  interface microstructure resulted in a remarkable improvement in damping over the all temperature range. Savaskan et al. (2021) investigated the effect of different heat treatment conditions on the mechanical properties of Zn-40Al-2Cu-2Si alloy. They found that heat treatment (T6) consisting of homogenization followed by quench-aging steps, increased the hardness and tensile strength of the as-cast alloy.

As a result, the addition of copper up to 3% increases the hardness and strength of Zn-Al-Cu alloys due to solid solution hardening, but the addition of copper exceeding 1% causes the problem of dimensional instability and low ductility due to the formation of metastable  $\epsilon$  ( $\text{CuZn}_4$ ) phase, and transformation of  $\epsilon$  phase into the stable T' ( $\text{Al}_4\text{Cu}_3\text{Zn}$ ) phase in the structure. Heat treatment is an effective method to eliminate these problems and obtain good structural and mechanical properties. Optimized structural and mechanical properties are vital in order to enhance the use of these alloys, which have many advantages compared to other non-ferrous metals. Therefore, low-copper addition was preferred to minimize dimensional stability and obtain balanced mechanical properties in this study. Moreover, the effect of heat treatment consisting of solution treatment and water quenching followed by aging at different periods on the structure and mechanical properties of Zn-27Al-1Cu alloy, especially on microstructural change and damping behaviour, was investigated.

## 2. Material and method

### 2. Materyal ve metot

Zn-27Al-1Cu alloy was produced by the gravity casting method using high-purity (99.9%) zinc, commercially pure (99.7%) aluminium, and Al-50Cu master alloys. The amount of alloying materials was calculated according to the weight ratios in the Zn-27Al-1Cu alloy system. These

alloys were melted in an electric furnace at 600 °C and then poured from 585 °C into a steel mould, which was manufactured as a conical shape with a bottom diameter of 45 mm, a top diameter of 60 mm and a length of 190 mm, after stirring for 5 min. Some of the ingots were subjected to heat treatment consisting of solutionizing, water-quenching and aging steps. The solutionizing process was carried out in an electric furnace at 380 °C for 24 hours followed by water-quenching. Quenching was done by rapid cooling with cold water. Artificial aging was performed in an air circulation oven at 100 °C for different durations ranging from 0.5 hours to 5 hours. As-cast and heat-treated ingots were mechanically processed to prepare metallography, tensile, hardness and V-notch impact samples as shown in Figure 1. Tensile specimens were prepared according to ASTM E8/M-11 standard with a gauge length of 25 mm and a diameter of 6 mm. The Charpy V-notch impact test specimens were manufactured according to ASTM E23 with dimensions of 10 mm  $\times$  10 mm  $\times$  55 mm. Hardness and metallography samples were machined with a diameter of 10 mm and a thickness of 10 mm. Tensile tests were carried out using a universal servo-hydraulic testing machine at a strain rate of  $1.3 \times 10^{-3} \text{ s}^{-1}$ . The elongation of the samples was recorded with the aid of a video extensometer. The hardness measurements were performed using a Brinell hardness tester with a 2.5 mm diameter ball indenter under a load of 31.25 kgf and a dwell time of 15 s. Charpy-impact tests were performed using damping test equipment with the maximum impact energy of 100 joules (J) and accuracy of  $\pm 0.5 \text{ J}$ . After the impact tests, the fracture surfaces of the impacted samples were observed with a scanning electron microscope (SEM). The as-cast and heat-treated samples of the alloy were prepared by standard metallography methods for microstructural examinations. They were then etched with 3% nital (3% nitric acid + 97% deionized water) solution to reveal their microstructures. Microstructural examinations of the samples were performed using both an optical microscope equipped with a digital camera and an SEM equipped with the energy-dispersive spectroscope, EDS. The average grain size of the heat-treated samples was calculated from their optical metallography images using an image processing software, ImageJ. To confirm the accuracy of the results, tensile, hardness and impact tests were repeated at least five times for all conditions and the average of the five measurements was taken.

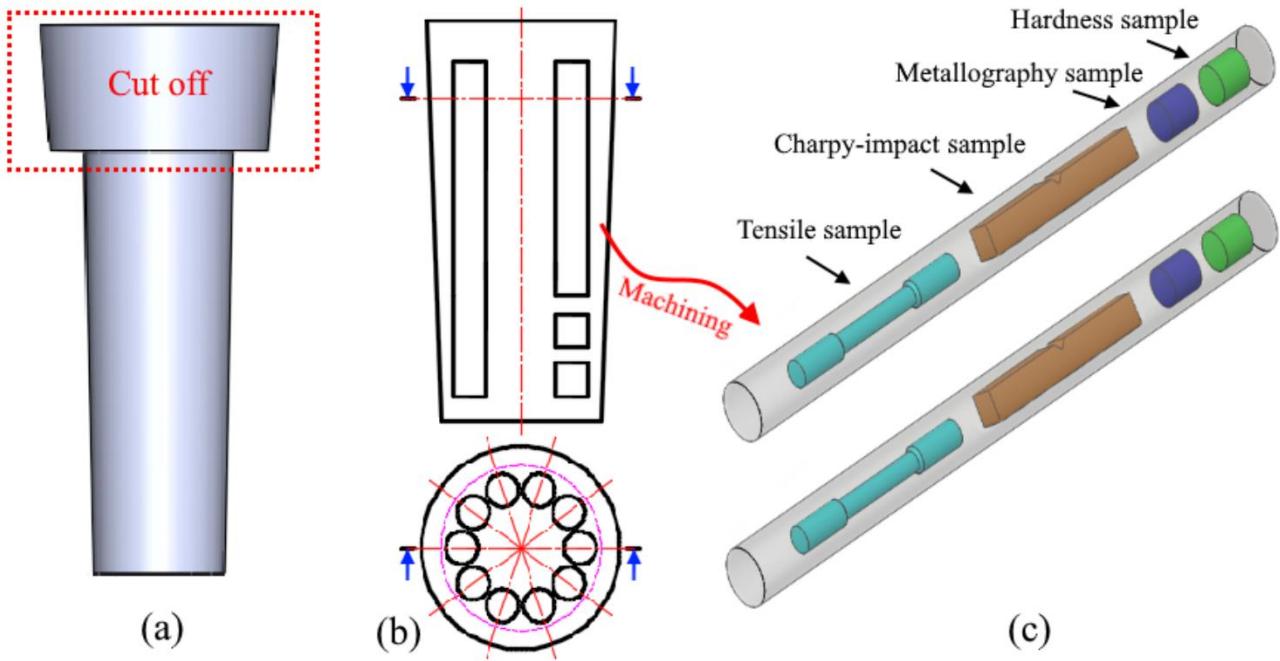


**Figure 1.** (a) The ingot form after casting, (b) Schematic representation of machining (c) Test specimens  
**Şekil 1.** (a) Döküm sonrası külçe formu, (b) Talaşlı imalatın şematik gösterimi (c) Test numuneleri

### 3. Discussion and conclusions

#### 3. Tartışma ve sonuçlar

#### 3.1. Microstructural studies

##### 3.1. Mikroyapısal incelemeler

Metallographic examination with an optic microscope in Figure 2(a) showed that the microstructure of as-cast alloy consisted of a typical dendritic structure consisting of micro-components, as a result of the final solidification. To determine the average composition of each phase, EDS analysis was performed from the regions marked in the SEM image of the as-cast alloy given in Figure 2(b). The average composition of  $\alpha$ ,  $\eta$ ,  $\epsilon$  and  $\beta$  phases in the as-cast alloy are listed in Table 1. The EDS results revealed that Zn-27Al-1Cu alloy consisted of aluminium-rich  $\alpha$  phase, zinc-rich  $\eta$ -phase, zinc-

rich eutectoid  $\beta$  phase and intermetallic  $\epsilon$  ( $\text{CuZn}_4$ ) phase. This dendritic and multiphase structure of the as-cast alloy was due to the thermal instabilities, typical of transient solidification, and the phase transformations during the cooling process. According to the binary phase diagram of Zn-Al alloys given in Ref. (Zhang et al., 2020), during the cooling stages of the liquid alloy with Zn-27Al composition, there are three typical phase transformation processes: crystallization of primary  $\alpha$  phase ( $L \rightarrow \alpha$ ), peritectic reaction ( $L + \alpha \rightarrow \beta$ ), and eutectoid reaction ( $\beta \rightarrow \alpha + \eta$ ). In addition, Savaşkan & Hekimoğlu (2014) was presented the phase diagram of the ternary Al-Zn-Cu alloy system at 350 °C. According to this phase diagram, the  $\beta$  phase includes  $\alpha$ ,  $\eta$  and  $\epsilon$  phases in the ternary alloy system with Zn-27Al-1Cu composition. The  $\beta$  phase transformation takes place as  $\beta \rightarrow \alpha + \eta + \epsilon$  during the solidification.

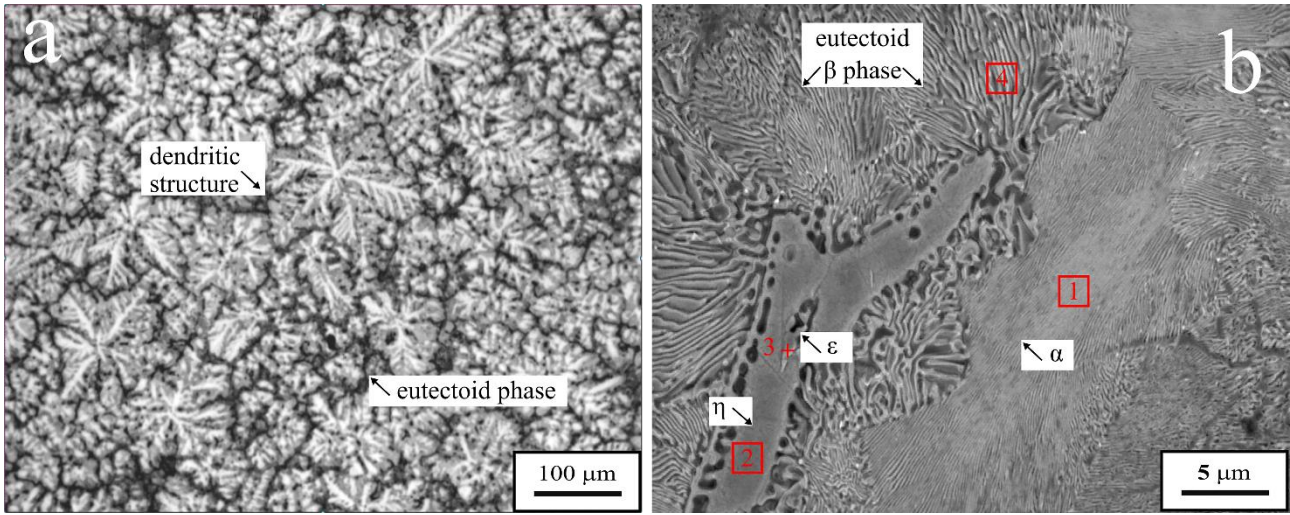


**Figure 2.** The microstructure of the as-cast alloy (a) optical microscope and (b) SEM image  
**Şekil 2.** Döküm alaşımının mikroyapısının (a) optik mikroskop ve (b) SEM görüntüsü

**Table 1.** EDS analyses of the points marked on the micrograph in Figure 2(b).  
**Tablo 1.** Şekil 2(b)'deki mikroyapıda işaretlenen noktaların EDS analizleri.

Position	Chemical composition with weight percent			
	Phase	Zn wt. %	Al wt. %	Cu wt. %
Point 1	$\alpha$	21.34	77.94	0.72
Point 2	$\eta$	85.06	12.56	2.38
Point 3	$\varepsilon$	85.09	1.26	13.65
Point 4	$\beta$	72.29	26.54	1.17

The microstructures of the heat-treated alloy under different aging duration observed with the optical microscope are given in Figure 3. The solution treatment followed by the quench-aging process removed the dendritic microstructure of the alloy and transformed it into a coarse-grained structure with the  $\beta$  matrix, containing precipitates within and through the grain boundaries, as seen in Figure 3(a-c). In addition, it was observed that the grain size increased with increasing aging duration and the number of precipitates located close to the grain boundaries increased. Zhao et al. (2018) indicated that the diffusion of solute atoms along the grain boundaries enhanced the grain growth in Al-Zn based alloys. The average grain size of the alloy aged for 0.5 hours, 2.5 hours and 5 hours was determined by an image processing software to be 145 $\mu\text{m}$ , 205  $\mu\text{m}$  and 245  $\mu\text{m}$ , respectively. The detailed SEM view of the grain boundary region of the alloy quench-aged for 2.5 hours, after solution treatment is given in Figure 3(d). From this figure, it is clearly seen that precipitates are formed within

the  $\beta$  matrix and along the grain boundaries. In addition, a cellular structure consisting of  $\alpha$  (dark) and  $\eta$  and  $\varepsilon$  (light) phase precipitates were formed along the grain boundaries. Moreover, EDS analysis revealed that the formation of  $T'$  phase ( $\text{Al}_4\text{Cu}_3\text{Zn}$ ), a product of four-phase transformation ( $\alpha+\varepsilon\rightarrow T'+\eta$ ), started in the structure. During the solution treatment at 380 °C for 24h, a large amount of  $\alpha$  and  $\eta$  phases dissolve, resulting in the formation of the supersaturated  $\beta$  phase. There are four phases  $\beta$ ,  $\eta$ ,  $\alpha$  and  $\varepsilon$  in the quenched alloy after solution treatment (Yang et al., 2013). After aging, especially in the early stages, the supersaturated  $\beta$  phase decomposed into the irregularly cellular structure through discontinuous reaction:  $\beta\rightarrow\alpha+\eta+\varepsilon$ . The progressive stage of aging activates the four-phase transformation ( $\alpha+\varepsilon\rightarrow T'+\eta$ ) and initiates the formation of the  $T'$  phase, where  $T'$  is the phase with higher stability than the  $\varepsilon$  phase (Chen et al., 2015; Ferreira-Palma et al., 2021).

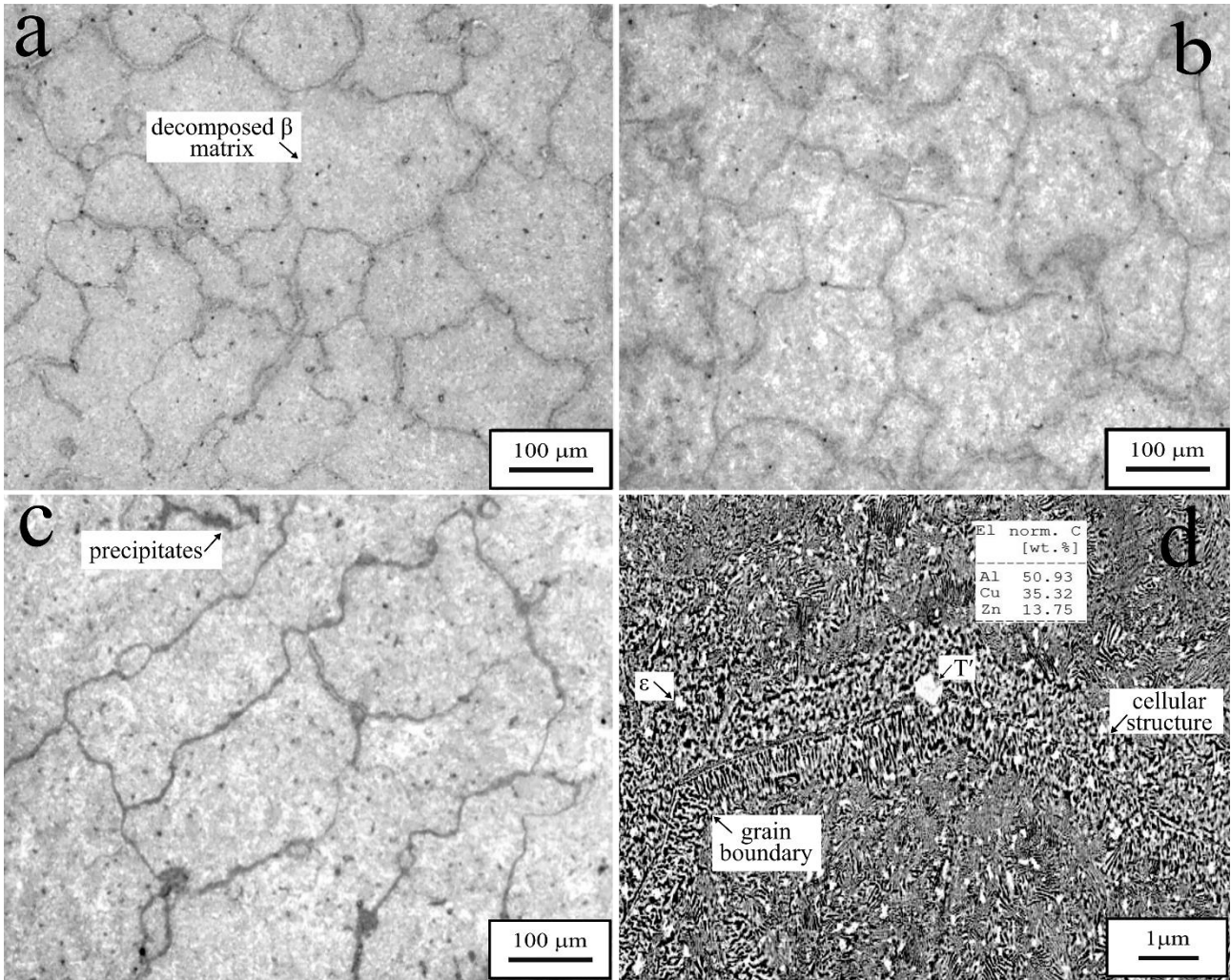


**Figure 3.** Optical microscope images of microstructure of the alloy aged for (a) 0.5 h, (b) 2.5 h, (C) 5 h and (d) SEM image of the grain boundary of the alloy aged for 2.5 h in detail.

**Şekil 3.** (a) 0,5 h, (b) 2,5 h, (C) 5 h yaşlandırılmış alaşımın mikroyapısının optik mikroskop görüntüleri ve (d) 2,5 saat yaşlandırılmış alaşımın tane sınırının ayrıntılı SEM görüntüsü

SEM analyses were performed at low and high magnifications to examine the microstructural change more comprehensively. The detailed SEM images of the microstructure of the alloy under as-cast and heat-treated conditions (aged for 2.5 h and aged for 5h) are given in Figure 4. Figure 4(a-b) shows the Al-rich  $\alpha$  dendritic arms, the Zn-rich ( $\alpha + \eta$ ) dendrites, the lamellar  $\beta$  phase, the Zn-rich  $\eta$  phase and the Cu-rich  $\epsilon$  phase, which formed in the microstructure of the alloy after solidification. During the solidification of as-cast alloy, the primary  $\alpha$  phase solidified firstly to form the cores of dendrites bordered by the eutectoid  $\beta$  phase.

Then, the lamellar  $\beta$  phase, which was formed as a result of the transformation of the  $\beta$  phase into  $\alpha$  and  $\eta$  phases by the eutectoid reaction during cooling, solidified. Finally, the  $\eta$  and  $\epsilon$  phases solidified in the inter-dendritic region. The copper-rich  $\epsilon$  phase (light-grey) is generally located within the lamellar  $\beta$  phase as seen in Figure 4(b). The fine lamellar structure represents the  $\alpha$  phase, while the coarse lamellar structure represents  $\beta$  ( $\alpha$  (dark) +  $\eta$  (light)) phase in Figure 4(b). [Savaşkan & Hekimoğlu \(2014\)](#) defined the  $\alpha + \eta$  (middle-grey) phase as  $\alpha$  core- $\beta$  dendrite, which is supported by the detail image of this phase in Figure 4(b).

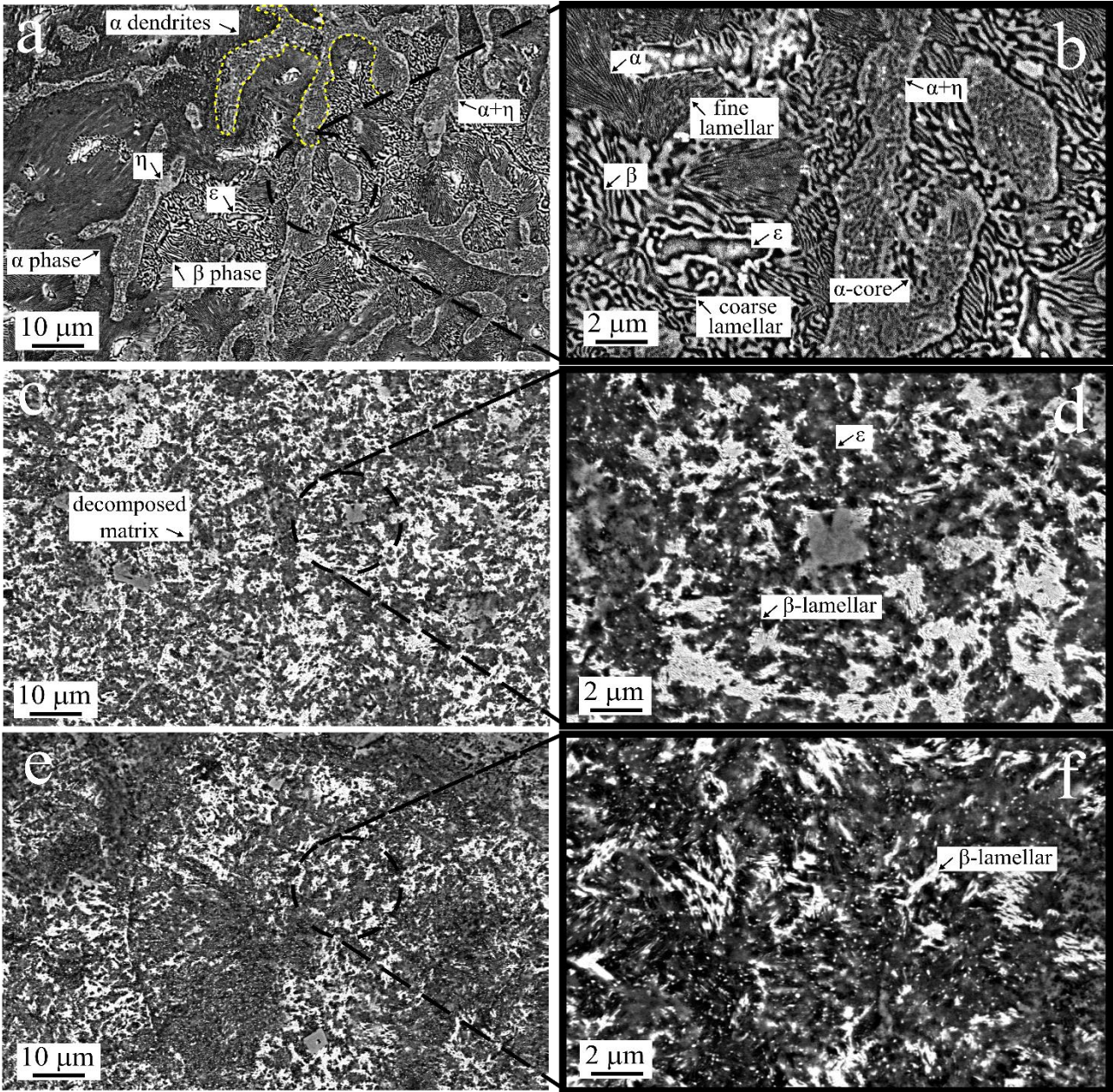


**Figure 4.** SEM image of microstructure of the Zn-27Al-1Cu alloy (a-b) as-cast and its detail, (c-d) aged for 2.5 h and its detail, (e-f) aged for 5 h and its detail.

**Şekil 4.** Zn-27Al-1Cu alaşımının mikroyapısının (a,b) döküm hali ve detayının, (c,d) 2,5 saat yaşlandırılmış ve detayının (e-f) 5 saat yaşlandırılmış ve detayının SEM görüntüsü

The microstructure of the alloy aged for 2.5 hours and aged for 5 hours are given in Figure 4(c-d) and Figure 4(e-f), respectively. As it is clearly seen in Figure 4(c),  $\alpha$  and  $\eta$  phases almost completely dissolved in each other through the heat treatment, and the dendritic microstructure turned into the decomposed matrix. The coarse lamellar structure turned into a fine lamellar structure after aging for 2.5 h, as seen in Figure 4(b-d). Moreover, heat treatment increased the dissolution of the  $\epsilon$  phase in the matrix, resulting in a more homogeneous structure with dispersed precipitates. The microstructure formed after casting resulted from

the solidification mechanism (Turhal & Savaşkan, 2003; Jeshvaghani et al., 2016). However, the microstructural changes of the alloy after heat treatment resulted from the solution treatment and aging-activated precipitation mechanisms. The structure of the quenched alloy after solution treatment consists mainly of the supersaturated  $\alpha$  phase and supersaturated  $\beta$  phase (Movahedi et al., 2019). In the early stage of aging (aged for 0.5 h), the supersaturated  $\beta$  phase transformed into a fine lamellar structure, which was formed within the grain. As the aging time increased, the large and coarse lamellar  $\beta$  phase decomposed by the

diffusion effect and transformed into a smaller and thinner lamellar structure. In other words, when the aging time increased from 2.5 hours to 5 hours, the  $\alpha$  phase became more prominent, while the  $\beta$  phase gradually disappeared (Figures 4(d-f)). This structural change is evident from the difference between the microstructure of the alloy aged for 2.5 h and the alloy aged for 5 h given in Figure 4. The microstructure of the as-cast alloy formed as a result of solidification and the microstructural changes after heat treatment are compatible with previous studies on similar Zn–Al based alloys (Yang et al., 2013; Chen et al. 2015; Jeshvaghani et al., 2016; Movahedi et al., 2019; Ferreira-Palma et al., 2021).

### 3.2. Mechanical properties

#### 3.2 Mekanik özellikler

Some mechanical properties of the Zn–27Al–1Cu alloy in both as-cast and different aging conditions are listed in Table 2. It is seen from the table that the hardness and tensile strength increase with increasing aging time up to 2.5 hours, but the percent elongation decrease. When the aging time reached 5 hours, hardness and tensile strength decreased while percent elongation increased significantly. The highest hardness and strength with the lowest percent elongation were obtained from the alloy aged for 2.5 hours. The change in hardness, strength and ductility values can be explained by the microstructural changes and precipitation hardening mechanism that occur as a result of the solution treatment followed by quenching and aging. After 0.5 hours of aging, the alloy showed a rapid increase in hardness and tensile strength together with a slight increase in percentage elongation. Hence, Zhang et al. (2020) reported that when the alloys were subjected to

short-term annealing in the single-phase region followed by water-quenching, the elongation was generally improved without decrements in the strength of the alloys. After the solution treatment and quenching, a supersaturated solid solution is obtained, which causes a large amount of distortion in the matrix, resulting in the improvement of the hardness and strength of the alloy. The increase in the hardness and strength of the alloy aged for 0.5 hours can be explained by this mechanism. However, a supersaturated solid solution is an unstable structure that is transformed into a stable structure by prolonged periods of aging. In addition, with increasing aging time, the precipitation of secondary phase particles becomes more active. This causes distortion in the matrix ( $\beta$ ) due to the coherence effect (Wei et al., 2021; Savaşkan et al., 2021). This restricts the movement of dislocations and makes it difficult to slide, which can be attributed to the increase in hardness and strength and decrease in elongation of the alloy aged for 2.5 hours. After the 5 hour aging period, the considerable decrease in the hardness and tensile strength of the alloy can be attributed to the over-aging behaviour. During the over-aging stage, the precipitates begin to lose the effect of coherency characteristic and the precipitates rapidly coalesce, grow and coarsen, which causes the elimination of barriers that restrict the dislocation movement. In general, prolonged aging processes can cause a decrease in strength due to decreased dislocation density and increased grain size (Yang et al., 2013; Meng et al., 2021). In addition, after 5 hours of aging period, the supersaturated  $\beta$  phase decomposed to a very fine lamellar structure, which contributed greatly to the improvement of the ductility of the alloy.

**Table 2.** Mechanical properties of the Zn–27Al–1Cu alloy in as-cast and heat treated conditions

**Tablo 2.** Dökülmüş ve ısıtılmış işlem görmüş durumdaki Zn–27Al–1Cu alaşımının mekanik özellikleri

Aged Condition	Tensile Strength (MPa)	Hardness (BHN)	Percentage Elongation (%)	Impact Energy (J)
As-cast	340	92	13	5.59
0.5 hours	385	105	17	5.82
2.5 hours	405	112	9	2.87
5 hours	315	84	36	2.96

On the other hand, impact energy was raised in the early stage of aging, thereafter it reduced dramatically with increasing aging duration and finally it raised slightly in the prolonged stage of the aging process. The highest impact energy, i.e. toughness was obtained from the 0.5 hours aged

alloy with well-balanced tensile strength and percent elongation. After 2.5 hours of aging period, the impact energy of the alloy decreased distinctly, which may be due to the high hardness of the alloy and the presence of the high number of fine-hard precipitates, which increase the tendency of crack

formation. The impact energy increased slightly after aging for 5 hours but was still low compared to the as-cast condition. This may be due to the fact that the ductility of the alloy aged for 5 hours was quite high, but the tensile strength was distinctly low. The change in damping capacity can be attributed to the mechanical properties combined with structural changes due to the aging process. Another important factor affecting the mechanical properties of the alloy is grain size. As the grain size increases, the total interface boundary decreases, hence a decrease in the total energy of the material, resulting in a reduction of the damping capacity (Zhongming et al., 2000; Zhang et al., 2006; Zhang et al., 2020). The overall decrease in the impact energy of the alloy with increasing aging time after 0.5 hours may be due to

the increase in grain size, as seen in Figure 3(a-c). However, analysis of fracture surfaces can also play a key role in explaining the change in the toughness of materials. Therefore, the fracture surfaces of the impact samples were examined by SEM after the impact tests. The mechanical properties of Zn-27Al-1Cu alloy in the as-cast and heat treatment conditions were compared with the mechanical properties of similar Zn-Al based alloys produced in previous studies, given in Table 3. The Zn-27Al-1Cu alloy exhibited better ductility in general than other alloys due to its low copper content. It also had moderate hardness and tensile strength compared to Zn-Al alloys with high Al and Cu content. However, it had a much better impact energy than the Zn-15Al-3Cu alloy.

**Table 3.** The comparison table of mechanical properties of some Zn-Al based alloys in as-cast and heat treatment conditions.

**Tablo 3.** Bazı Zn-Al esaslı alaşımların döküm ve ısı işlem koşullarındaki mekanik özelliklerinin karşılaştırma tablosu.

Alloy composition (wt. %)	Process status	Hardness (BHN)	Tensile strength (MPa)	Percent elongation (%)	Impact energy (J)	References
Zn-27.5Al-1Cu	As-cast	92	340	13	5.59	Present study
	S:380 °C, 24h+ WQ A:100 °C, 2.5h	112	405	9	2.87	
Zn-27.5Al-2.5Cu-0.03Mg	As-cast	130	325	3	-	Prasad (2004)
	S: 360 °C, 12h + WQ A:180 °C, 2h	118	290	3.8	-	
Zn-25Al-3Cu	As-cast	92	350	8	-	Jovanović et al. (2007)
	S: 370 °C, 3h + WQ	105	360	24	-	
Zn-28.5Al-2.5Cu-0.012Mg	As-cast	138	318	2.4	-	Babic et al. (2010)
	S:370 °C, 3h+WQ A: RT, 34 days	121	301	5.2	-	
Zn-27Al-2Cu-0.012Mg	As-cast	155	490	3	-	Yang et al. (2013)
	S:365 °C, 1 h + WQ A:140 °C, 12 h	108	316	26.5	-	
Zn-15Al-3Cu	As-cast	83 <sub>HRF</sub>	304	3.1	2	Savaşkan & Hekimoğlu (2014)
	S:330 °C, + WQ A:180 °C, 210s	95 <sub>HRF</sub>	406	3	-	
Zn-25Al-3Cu-1Si	As-cast	67 <sub>HRB</sub>	364	2,2	-	Savaşkan et al. (2015)
	S:350 °C, 36h + WQ A:150 °C, 2min.	84.5 <sub>HRB</sub>	490	3,1	-	
Zn-40Al-2Cu	As-cast	94.3 <sub>HRF</sub>	340	1.8	-	Bican & Savaşkan (2020)
	A:150°C, 24h	86.3 <sub>HRF</sub>	291	3.1	-	
Zn-40Al-2Cu-2Si	As-cast	126	375	1.4	-	Savaşkan et al. (2021)
	S:375 °C, 36 h + WQ A:180 °C, 2 min	174	475	1	-	

S: solution treatment, WQ: water-quenching, A: aging, HRB: Rockwell B, HRF: Rockwell F

### 3.3. Fracture characteristic

#### 3.3. Kırılma karakteristiği

The fracture surface images of the impact samples obtained from both as-cast and aged alloy were given in Figure 5(a-d). The impact fracture surface

of the as-cast alloy was quite rough and exhibited brittle fracture characteristics with cleavage crack on the margin of the plane of brittle fracture, as seen in Figure 5(a). Zn–Al based alloys especially in the as-cast state exhibit brittle fracture characteristics due to the residual stresses and dimensional instability caused by the non-equilibrium cooling rates of the alloying elements (Turhal and Savaşkan, 2003; Hasan et al., 2020). Dimensional instabilities and residual stresses, which cause brittle fractures in the structure could be considerably eliminated by prolonged aging after solution treatment (Chen et al., 2008; Zhang et al., 2020; Meng et al., 2021). However, the brittle fracture tendency continued with the precipitation of secondary-phase particles in the early stages and progressive stage of aging. As a matter of fact, brittle fracture behaviour with a large cleavage plane was observed in the alloy aged for 0.5 h. In Figure 5(b), the fracture surface had a large cleavage plane but no large fracture cracks, indicating that the plastic deformation ability of the alloy aged for 0.5 h was relatively better than as-cast alloy. In fact, the alloy aged for 0.5 h exhibited

better ductility and impact energy than the as-cast alloy. It was observed that a highly brittle fracture mode occurred in the alloy aged for 2.5 hours, where maximum hardness and strength were obtained. This fracture surface consisted of largely deformed regions along with many cracks, as seen in Figure 5(c). This may be due to the local stresses created by numerous dispersed precipitates (Zn-rich and Cu-rich) in the matrix, increasing the tendency of crack formation and crack propagation (Wei et al., 2021). In the alloy aged for 5 hours, it was observed that the fracture surface consisted of numerous dimples, which is a characteristic feature of the ductile fracture behaviour, as seen in Figure 5(d). This ductile fracture mode in the alloy, which is aged for a long time, may be due to its high percent elongation. In addition, the transformation of the coarse lamellar  $\beta$  phase into the fine lamellar structure after the prolonged aging process may have greatly contributed to the improvement of the plasticity of the alloy (Yang et al., 2013; Zhang et al., 2020). As a result, brittle fracture mode transformed into ductile fracture mode after prolonged aging condition as seen in Figure 5(c-d).

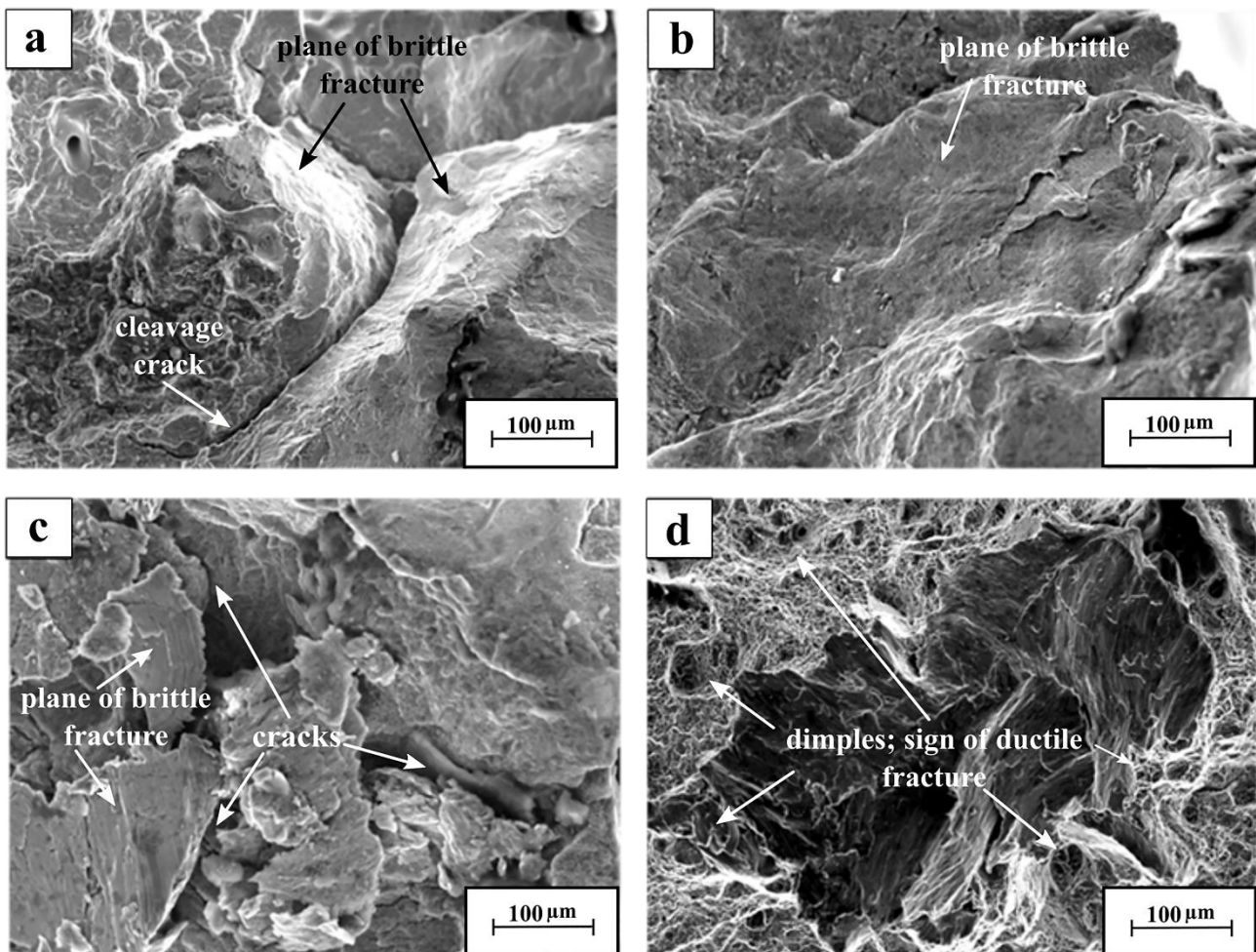


**Figure 5.** SEM images showing impact fracture surfaces of the alloy in as-cast and different aging periods: (a) as-cast, (b) aged for 0.5 h, (c) aged for 2.5 h, (d) aged for 5 h

**Şekil 5.** Döküm ve farklı yaşlandırma periyotlarında, alaşımın darbeli kırılma yüzeylerini gösteren SEM görüntüleri: (a) dökülmüş, (b) 0,5 h yaşlandırılmış, (c) 2,5 h yaşlandırılmış, (d) 5 h yaşlandırılmış

#### 4. Conclusion

##### 4. Sonuçlar

The effects of different aging periods on the microstructural behaviour and impact characteristic of the Zn-27Al-1Cu alloy were examined. The results are summarized as follows. The as-cast alloy consisted of the  $\alpha$  (Al-rich) dendrites surrounded by the eutectoid  $\beta$  (Al and Zn-rich) phase, and  $\eta$  (Zn-rich) phase and metastable  $\epsilon$  (Cu-rich) phase. The solution treatment followed by the quench-aging process completely eradicated the dendritic microstructure resulting from solidification. Heat treatment provided the dendritic microstructure to transform into a highly homogeneous coarse-grained structure containing fine precipitates. The aging process directly affected the mechanical properties of the alloy. The best combination of strength and ductility properties was attained from the aged alloy for 0.5 hours. The highest impact energy was exhibited in the aged alloy for 0.5 hours, while the lowest impact energy was exhibited in the aged alloy for 2.5 hours. The variation in damping behaviour resulted from the change in microstructural and mechanical properties and, precipitation hardening mechanism due to aging treatment. The prolonged aging process transformed the brittle fracture characteristic of the cast alloy into a relatively ductile fracture characteristic.

#### Acknowledgement

##### Teşekkürler

The initial version of this article was presented in the International Online Conferences on Engineering and Natural Sciences (IOCENS'21) proceedings held on 05-07 July 2021, in Gümüşhane, TURKEY.

#### Author contribution

##### Yazar katkısı

Fatih ŞENASLAN: Methodology, conceptualization, investigation, data collection and analysis, writing—original draft, visualization. Murat AYDIN: Conceptualization, supervisor, work administration, writing—review and editing.

#### Declaration of ethical code

##### Etik beyanı

In this study, we undertake that all the rules that must be followed within the scope of the "Higher Education Institutions Scientific Research and

Publication Ethics Directive" have been complied with, and that none of the actions specified under the title of "Actions Contrary to Scientific Research and Publication Ethics" have been carried out.

The authors of this article declare that the materials and methods used in this study do not require ethical committee approval and/or legal-specific permission.

#### Conflicts of interest

##### Çıkar çatışması beyanı

The authors declare that there is no conflict of interest.

#### References

##### Kaynaklar

- Anjan, B. N., & Kumar, G. P. (2019). Wear behaviour of ZA27-based composite reinforced with 5 wt% of SiC particles and processed by multi-directional forging. *Transactions of the Indian Institute of Metals*, 72(6), 1621-1625. <https://doi.org/10.1007/s12666-019-01705-0>
- Aydın, M. (2012). High-cycle fatigue behavior of severe plastically deformed binary Zn-60Al alloy by equal-channel angular extrusion. *Journal of Materials Processing Technology*, 212(8), 1780-1789. <https://doi.org/10.1016/j.jmatprotec.2012.03.027>
- Aydın, M., & Şenaslan, F. (2018). The effect of quench-aging on the mechanical properties of Zn-27Al-1Cu alloy. *International Journal of Materials Research*, 109(8), 699-707. <https://doi.org/10.3139/146.111665>
- Babic, M., Mitrovic, S., & Jeremic, B. (2010). The influence of heat treatment on the sliding wear behavior of a ZA-27 alloy. *Tribology international*, 43(1-2), 16-21. <https://doi.org/10.1016/j.triboint.2009.04.016>
- Bican, O., & Savaşkan, T. (2020). Influence of T5 heat treatment on the microstructure and lubricated wear behavior of ternary ZnAl40Cu2 and quaternary ZnAl40Cu2Si2. 5 alloys. *Materialwissenschaft und Werkstofftechnik*, 51(3), 383-390. <https://doi.org/10.1002/mawe.201800222>
- Chen, T. J., Yuan, C. R., Fu, M. F., Ma, Y., Li, Y. D., & Hao, Y. (2008). In situ silicon particle reinforced ZA27 composites: Part 1—Microstructures and tensile properties. *Materials Science and Technology*, 24(11), 1321-1332. <https://doi.org/10.1179/174328408X295971>

- Chen, T. J., Zhao, H. J., Ma, Y., & Hao, Y. (2015). Microstructure Observation of Naturally Aged Thixoforming ZA27 Alloy. *Materials Research*, 18, 1322-1330. <https://doi.org/10.1590/1516-1439.050015>
- Choudhury, P., Das, S., & Datta, B. K. (2002). Effect of Ni on the wear behavior of a zinc-aluminum alloy. *Journal of Materials Science*, 37(10), 2103-2107. <https://doi.org/10.1023/A:1015297904125>
- Ferreira-Palma, C., Dorantes-Rosales, H. J., López-Hirata, V. M., & Torres-Castillo, A. A. (2021). Effect of Ag additions on the microstructure and phase transformations of Zn-22Al-2Cu (wt.%) alloy. *International Journal of Materials Research*, 112(2), 108-117. <https://doi.org/10.1515/ijmr-2020-8009>
- Hasan, M. M., Sharif, A., & Gafur, M. A. (2020). Characteristics of eutectic and near-eutectic Zn-Al alloys as high-temperature lead-free solders. *Journal of Materials Science: Materials in Electronics*, 31(2), 1691-1702. <https://doi.org/10.1007/s10854-019-02687-x>
- Hernández-Rivera, J. L., Flores, E. E. M., Contreras, E. R., Rocha, J. G., de Jesus Cruz-Rivera, J., & Torres-Villaseñor, G. (2017). Evaluation of hardening and softening behaviors in Zn-21Al-2Cu alloy processed by equal channel angular pressing. *Journal of Materials Research and Technology*, 6(4), 329-333. <https://doi.org/10.1016/j.jmrt.2017.06.006>
- Jeshvaghani, R. A., Ghahvechian, H., Pirnajmeddin, H., & Shahverdi, H. R. (2016). Influence of heat treatment on the microstructure and wear behavior of end-chill cast Zn-27Al alloys with different copper content. *Applied Physics A*, 122(4), 397. <https://doi.org/10.1007/s00339-016-9820-5>
- Jovanović, M. T., Bobić, I., Djurić, B., Grahovac, N., & Ilić, N. (2007). Microstructural and sliding wear behaviour of a heat-treated zinc-based alloy. *Tribology Letters*, 25(3), 173-184. <https://doi.org/10.1007/s11249-006-9106-8>
- Kai, W., Baiqing, X., Yongan, Z., Guojun, W., Xiwu, L., Zhihui, L., & Hongwei, L. (2017). Microstructure evolution of a high zinc containing Al-Zn-Mg-Cu alloy during homogenization. *Rare Metal Materials and Engineering*, 46(4), 928-934. [https://doi.org/10.1016/S1875-5372\(17\)30124-8](https://doi.org/10.1016/S1875-5372(17)30124-8)
- Krupiński, M., Krol, M., Krupińska, B., Mazur, K., & Labisz, K. (2018). Influence of Sr addition on microstructure of the hypereutectic Zn-Al-Cu alloy. *Journal of Thermal Analysis and Calorimetry*, 133(1), 255-260. <https://doi.org/10.1007/s10973-018-7397-2>
- Liu, S., Tu, H., Wu, C., Wang, J., & Su, X. (2021). Effect of Silicon and Titanium on the Microstructure and Mechanical Properties of ZA12 Alloy. *Materials Today Communications*, 102564. <https://doi.org/10.1016/j.mtcomm.2021.102564>
- Mao, F., Chen, F., Yan, G., Wang, T. & Cao, Z. (2015). Effect of strontium addition on silicon phase and mechanical properties of Zn-27Al-3Si alloy. *Journal of Alloys and Compounds*, 622, 871-879. <https://doi.org/10.1016/j.jallcom.2014.11.013>
- Meng, X., Zhang, D., Zhang, W., Qiu, C., Liang, G., & Chen, J. (2021). Influence of solution treatment on microstructures and mechanical properties of a naturally-aged Al-27Zn-1.5 Mg-1.2 Cu-0.08 Zr aluminum alloy. *Materials Science and Engineering: A*, 802, 140623. <https://doi.org/10.1016/j.msea.2020.140623>
- Movahedi, N., Murch, G. E., Belova, I. V., & Fiedler, T. (2019). Effect of heat treatment on the compressive behavior of zinc alloy ZA27 syntactic foam. *Materials*, 12(5), 792. <https://doi.org/10.3390/ma12050792>
- Nagavelly, S., Velagapudi, V., & Narasaiah, N. (2017). Mechanical properties and dry sliding wear behaviour of molybdenum disulphide reinforced zinc-aluminium alloy composites. *Transactions of the Indian Institute of Metals*, 70(8), 2155-2163. <https://doi.org/10.1007/s12666-017-1037-6>
- Owoeye, S. S., Folorunso, D. O., Oji, B., & Borisade, S. G. (2019). Zinc-aluminum (ZA-27)-based metal matrix composites: a review article of synthesis, reinforcement, microstructural, mechanical, and corrosion characteristics. *The International Journal of Advanced Manufacturing Technology*, 100(1-4), 373-380. <https://doi.org/10.1007/s00170-018-2760-9>
- Pola, A., Tocci, M., & Goodwin, F. E. (2020). Review of microstructures and properties of zinc alloys. *Metals*, 10(2), 253. <https://doi.org/10.3390/met10020253>
- Prasad, B. K. (2004). Influence of heat treatment parameters on the lubricated sliding wear behaviour of a zinc-based alloy. *Wear*, 257(11), 1137-1144. <https://doi.org/10.1016/j.wear.2004.07.006>
- Pürçek, G. (2005). Improvement of mechanical properties for Zn-Al alloys using equal-channel angular pressing. *Journal of Materials Processing Technology*, 169(2), 242-248. <https://doi.org/10.1016/j.jmatprotec.2005.03.012>

- Rollez, D., Pola, A., Montesano, L., Brisotto, M., De Felicis, D., & Gelfi, M. (2017). Effect of aging on microstructure and mechanical properties of ZnAl15Cu1 alloy for wrought applications. *International Journal of Materials Research*, 108(6), 447-454. <https://doi.org/10.3139/146.111502>
- Savaskan, T., Aydın, M., & Odabaşoğlu, H. A. (2001). Fatigue behaviour of Zn-Al casting alloys. *Materials Science and Technology*, 17(6), 681. <https://doi.org/10.1179/026708301101510393>
- Savaşkan, T., & Hekimoğlu, A. P. (2014). Microstructure and mechanical properties of Zn-15Al-based ternary and quaternary alloys. *Materials Science and Engineering: A*, 603, 52-57. <https://doi.org/10.1016/j.msea.2014.02.047>
- Savaşkan, T., Pürçek, G., & Murphy, S. (2002). Sliding wear of cast zinc-based alloy bearings under static and dynamic loading conditions. *Wear*, 252(9-10), 693-703. [https://doi.org/10.1016/S0043-1648\(01\)00876-6](https://doi.org/10.1016/S0043-1648(01)00876-6)
- Ting, L. I. U., Si, N. C., Liu, G. L., Zhang, R., & Qi, C. Y. (2016). Effects of Si addition on microstructure, mechanical and thermal fatigue properties of Zn-38Al-2.5 Cu alloys. *Transactions of Nonferrous Metals Society of China*, 26(7), 1775-1782. [https://doi.org/10.1016/S1003-6326\(16\)64290-5](https://doi.org/10.1016/S1003-6326(16)64290-5)
- Turhal, M. Ş. & Savaşkan, T. (2003). Relationships between secondary dendrite arm spacing and mechanical properties of Zn-40Al-Cu alloys. *Journal of Materials Science*, 38(12), 2639-2646. <https://doi.org/10.1023/A:1024434602540>
- Vencl, A., Šljivić, V., Pokusová, M., Kandeve, M., Sun, H., Zadorozhnaya, E., & Bobić, I. (2021). Production, Microstructure and Tribological Properties of Zn-Al/Ti Metal-Metal Composites Reinforced with Alumina Nanoparticles. *International Journal of Metalcasting*, 1-10. <https://doi.org/10.1007/s40962-020-00565-5>
- Wei, S. L., Feng, Y., Zhang, H., Xu, C. T., & Wu, Y. (2021). Influence of aging on microstructure, mechanical properties and stress corrosion cracking of 7136 aluminum alloy. *Journal of Central South University*, 28(9), 2687-2700. <https://doi.org/10.1007/s11771-021-4802-y>
- Yang, C. F., Pan, J. H., & Lee, T. H. (2009). Work-softening and anneal-hardening behaviors in fine-grained Zn-Al alloys. *Journal of Alloys and Compounds*, 468(1-2), 230-236. <https://doi.org/10.1016/j.jallcom.2008.01.067>
- Yang, L. I. U., Li, H. Y., Jiang, H. F., & Lu, X. C. (2013). Effects of heat treatment on microstructure and mechanical properties of ZA27 alloy. *Transactions of Nonferrous Metals Society of China*, 23(3), 642-649. [https://doi.org/10.1016/S1003-6326\(13\)62511-X](https://doi.org/10.1016/S1003-6326(13)62511-X)
- Zhang, J., Wang, Q., Jiao, Z., Cui, C., Yin, F., & Yao, C. (2020). Effects of combined use of inoculation and modification heat treatment on microstructure, damping and mechanical properties of Zn-Al eutectoid alloy. *Materials Science and Engineering: A*, 790, 139740. <https://doi.org/10.1016/j.msea.2020.139740>
- Zhang, Y., Yang, L., Zeng, X., Zheng, B., & Song, Z. (2013). The mechanism of anneal-hardening phenomenon in extruded Zn-Al alloys. *Materials & Design*, 50, 223-229. <https://doi.org/10.1016/j.matdes.2013.02.069>
- Zhao, H., De Geuser, F., da Silva, A. K., Szczepaniak, A., Gault, B., Ponge, D., & Raabe, D. (2018). Segregation assisted grain boundary precipitation in a model Al-Zn-Mg-Cu alloy. *Acta Materialia*, 156, 318-329. <https://doi.org/10.1016/j.actamat.2018.07.003>
- Zhongming, Z., Jincheng, W., Gencang, Y., & Yaohe, Z. (2000). Microstructural evolution of the supersaturated ZA27 alloy and its damping capacities. *Journal of Materials Science*, 35(13), 3383-3388. <https://doi.org/10.1023/A:1004885002887>
- Zhu, Y. H., To, S., Liu, X. M., & Lee, W. B. (2006). Microstructural changes inside the lamellar structures of alloy ZA27. *Materials Characterization*, 57(4-5), 326-332. <https://doi.org/10.1016/j.matchar.2006.02.009>